Supplementary Information:

Bulk single crystal growth and optoelectronic properties of the quasi-two-dimensional perovskites $(CH_3NH_3)_3Bi_2X_9$ (X^-=Br^- and I^-)

Zhiyuan Li,[a] Xiangjun Wang,[a] Peng Zhao,[b] Jingquan Liu,[a,] and Xiangxin Tian[a,*]*

[a.] School of Materials and Engineering, Linyi University, Linyi 276000, China.

[b.] Sinoma Synthetic Crystals Co., Ltd., Beijing 100018, China.

Figure S1. The EDS measurement results of (a) $MA_3Bi_2Br_9$, (b) $MA_3Bi_2(Br_{0.74}I_{0.26})_9$, (c) $MA_3Bi_2(Br_{0.62}I_{0.38})_9$, and (d) $MA_3Bi_2I_9$, respectively.

Figure S2. XPS measurement results of $MA_3Bi_2Br_9$ single crystals. (a) The XPS survey of the crystal. (b)-(e) show the peaks of C, N, Bi, and Br elements, respectively.

Figure S3. XPS measurement results of $MA_3Bi_2(Br_{0.74}I_{0.26})_9$ single crystals. (a) The XPS survey of the crystal. (b)-(f) show the peaks of C, N, Bi, Br, and I elements, respectively.

Figure S4. XPS measurement results of $MA_3Bi_2(Br_{0.62}I_{0.38})_9$ single crystals. (a) The XPS survey of the crystal. (b)-(f) show the peaks of C, N, Bi, Br, and I elements, respectively.

Figure S5. XPS measurement results of $MA_3Bi_2I_9$ single crystals. (a) The XPS survey of the crystal. (b)-(e) show the peaks of C, N, Bi, and I elements, respectively.

Figure S6. Crystal structure of $MA_3Bi_2(Br_{0.62}I_{0.38})_9$ at room temperature. (a) presents the corner-shared connection of the $[Bi(Br/I)_6]^{3-}$ anionic groups in the structural framework. (b) The quasi-two-dimensional structure of $MA_3Bi_2(Br_{0.6}2I_{0.38})9$. (c) Ball-and-stick diagrams of the $[Bi(Br/I)_6]^{3-}$ octahedra with the bond-lengths labelled.

Figure S7. DSC measurements of (a) $MA_3Bi_2(Br_{0.74}I_{0.26})_9$, (b) $MA_3Bi_2(Br_{0.62}I_{0.38})_9$, and (c) $MA_3Bi_2I_9$ crystals within low-temperature range of the -120~20 ^oC, respectively.

Figure S8. Photos of the as-grown and aged (90 days) single crystals of $MA_3Bi_2Br_9$, $MA_3Bi_2(Br_{0.74}I_{0.26})_9$, and $MA_3Bi_2(Br_{0.62}I_{0.38})_9$, with the environmental relative humidity of RH 80%, respectively.

Figure S9. Photoluminescence excitation spectrum of $MA_3Bi_2Br_9$.

Figure S10. Mass attenuation coefficients of $MA_3Bi_2Br_9$, $MA_3Bi_2(Br_{0.62}I_{0.38})_9$, $MA_3Bi_2I_9$, and some other typical perovskite crystals. Insert present the detailed attenuation coefficients of the crystals.

Table S1. XPS results of the targeted $MA_3Bi_2X_9$ single crystals.

Table S2. Atomic coordinates ($\times 10^4$) and equivalent isotropic displacement parameters ($Å^2 \times 10^3$) for $MA_3Bi_2Br_9$.

Table S3. Atomic coordinates ($\times 10^4$) and equivalent isotropic displacement parameters ($Å^2 \times 10^3$) for $MA_3Bi_2(Br_{0.62}I_{0.38})_9$.

Table S4. Bond lengths [Å] and angles [°] for $MA_3Bi_2Br_9$.

Table S5. Bond lengths [Å] and angles [°] for $MA_3Bi_2(Br_{0.62}I_{0.38})_9$.

Table S6. Anisotropic displacement parameters ($Å^2 \times 10^3$) for $MA_3Bi_2Br_9$.

Table S7. Anisotropic displacement parameters ($Å^2 \times 10^3$) for $MA_3Bi_2(Br_{0.62}I_{0.38})_9$.

Table S8. Bond valence of Bi cations and the distortion parameter Δd of $[BiBr_6]^{3-}$ octahedra in $MA_3Bi_2Br_9$.

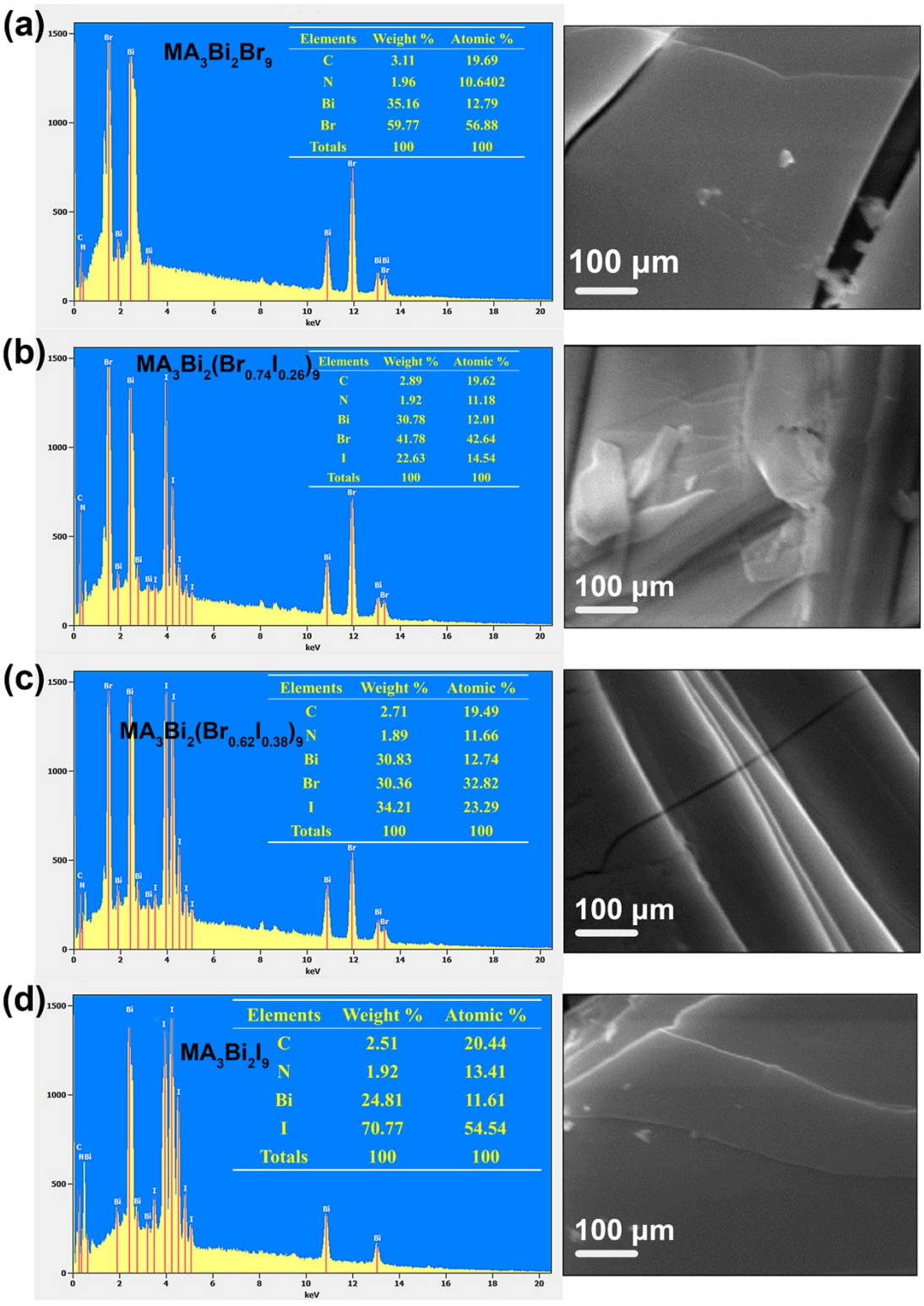

Figure S1. The EDS measurement results of (a) $MA_3Bi_2Br_9$, (b) $MA_3Bi_2(Br_{0.74}I_{0.26})_9$, (c) $MA_3Bi_2(Br_{0.62}I_{0.38})_9$, and (d) $MA_3Bi_2I_9$, respectively.

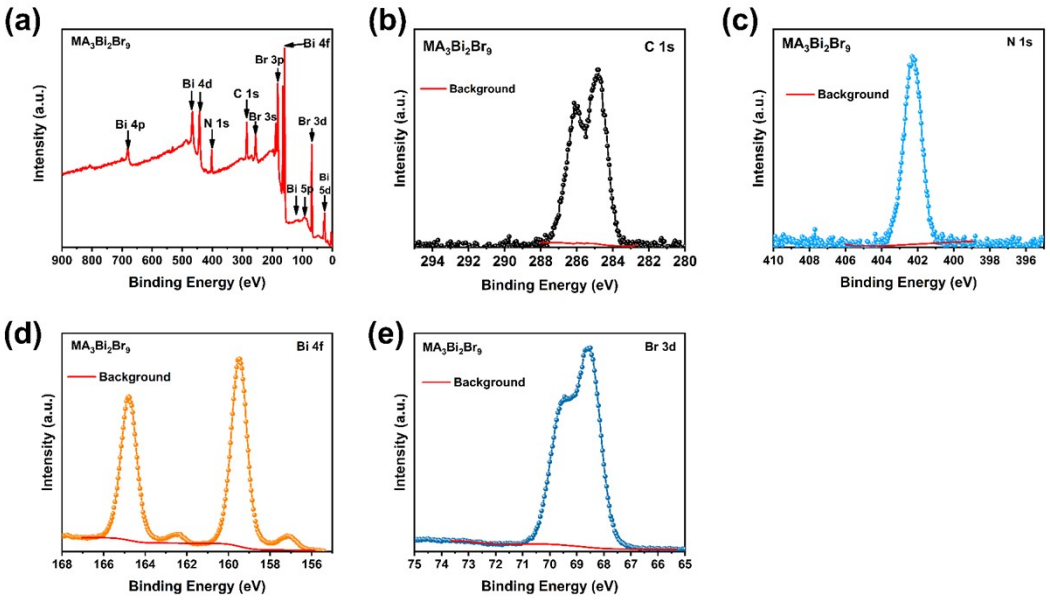

Figure S2. XPS measurement results of $MA_3Bi_2Br_9$ single crystals. (a) The XPS survey of the crystal. (b)-(e) show the peaks of C, N, Bi, and Br elements, respectively.

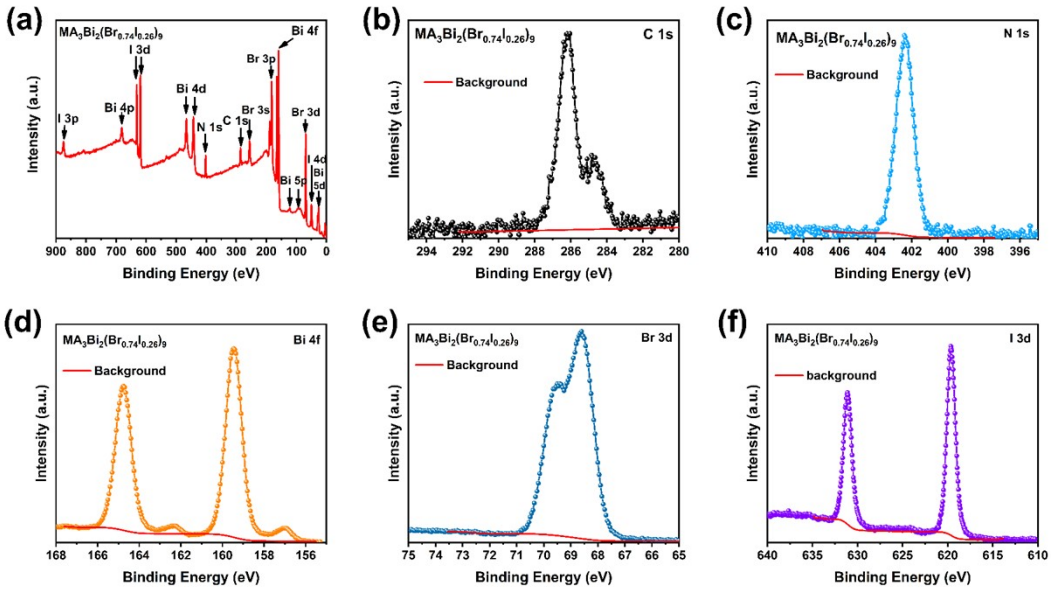

Figure S3. XPS measurement results of $MA_3Bi_2(Br_{0.74}I_{0.26})_9$ single crystals. (a) The XPS survey of the crystal. (b)-(f) show the peaks of C, N, Bi, Br, and I elements, respectively.

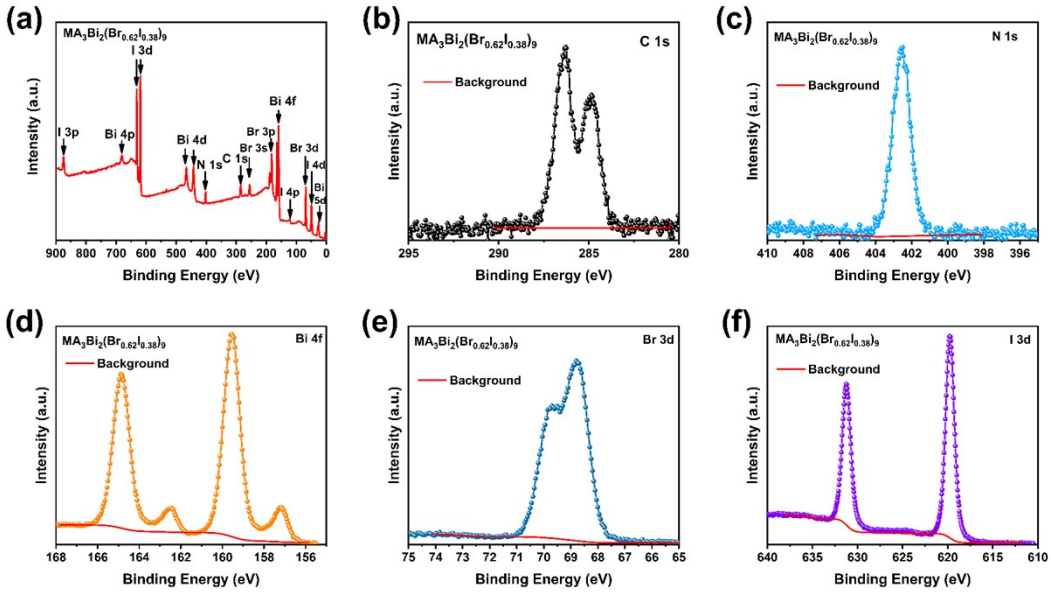

Figure S4. XPS measurement results of $MA_3Bi_2(Br_{0.62}I_{0.38})_9$ single crystals. (a) The XPS survey of the crystal. (b)-(f) show the peaks of C, N, Bi, Br, and I elements, respectively.

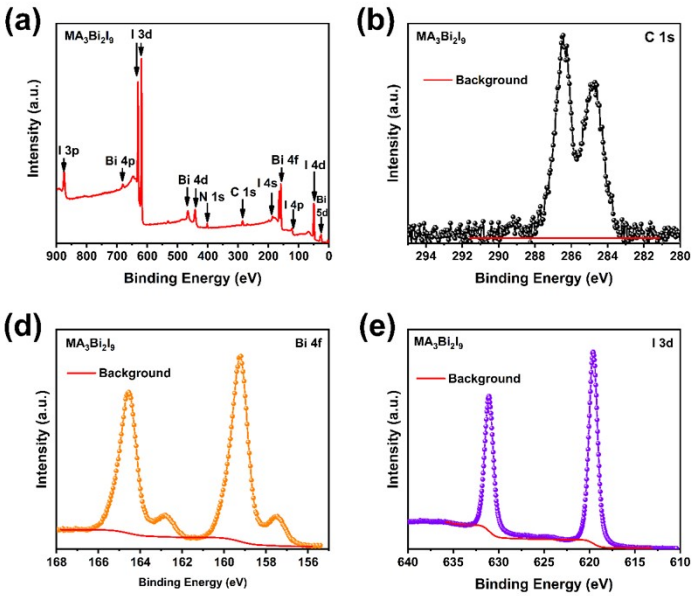

Figure S5. XPS measurement results of $MA_3Bi_2I_9$ single crystals. (a) The XPS survey of the crystal. (b)-(e) show the peaks of C, N, Bi, and I elements, respectively.

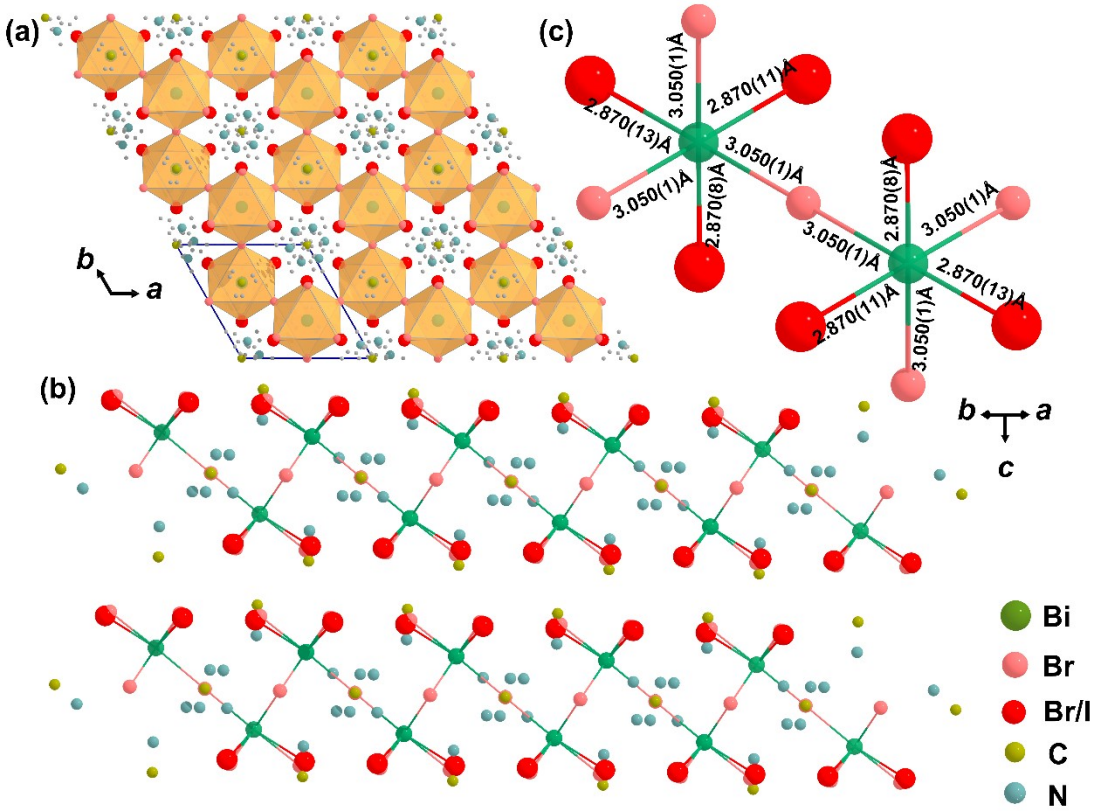

Figure S6. Crystal structure of $MA_3Bi_2(Br_{0.62}I_{0.38})_9$ at room temperature. (a) presents the corner-shared connection of the $[Bi(Br/I)_6]^{3-}$ anionic groups in the structural framework. (b) The quasi-two-dimensional structure of $MA_3Bi_2(Br_{0.6}2I_{0.38})9$. (c) Ball-and-stick diagrams of the $[Bi(Br/I)_6]^{3-}$ octahedra with the bond-lengths labelled.

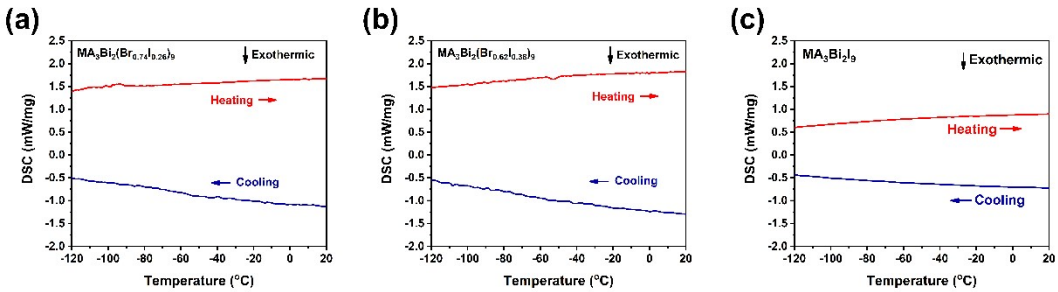

Figure S7. DSC measurements of (a) $MA_3Bi_2(Br_{0.74}I_{0.26})_9$, (b) $MA_3Bi_2(Br_{0.62}I_{0.38})_9$, and (c) $MA_3Bi_2I_9$ crystals within low-temperature range of the -120~20 °C, respectively.

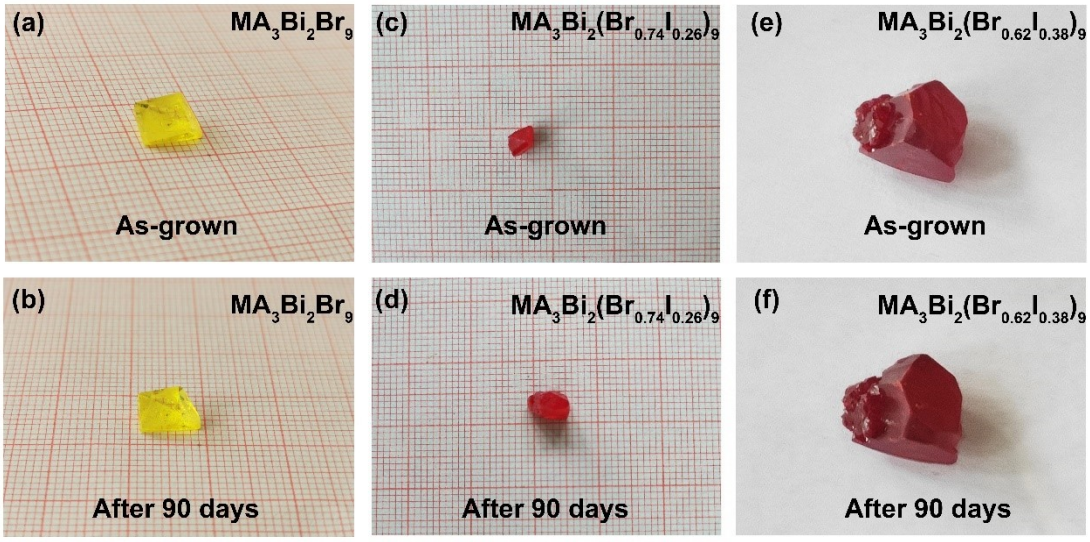

Figure S8. Photos of the as-grown and aged (90 days) single crystals of $MA_3Bi_2Br_9$, $MA_3Bi_2(Br_{0.74}I_{0.26})_9$, and $MA_3Bi_2(Br_{0.62}I_{0.38})_9$, with the environmental relative humidity of RH 80%, respectively.

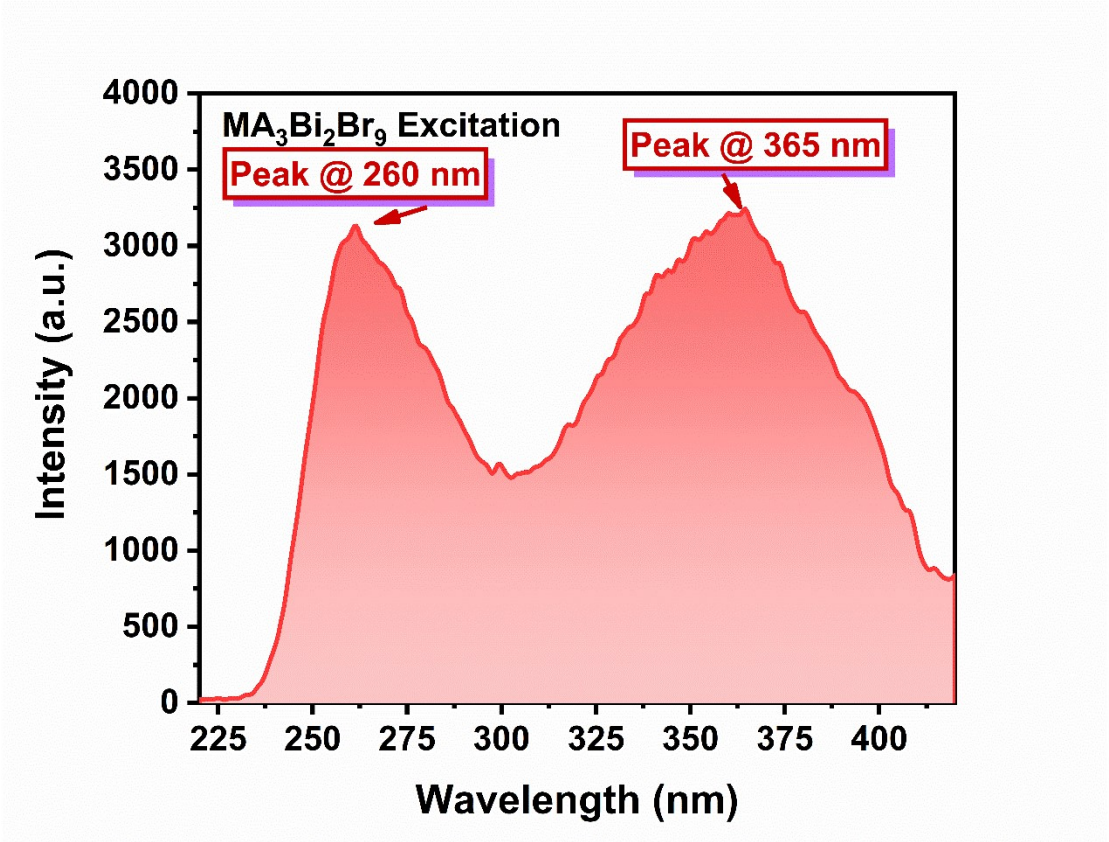

Figure S9. Photoluminescence excitation spectrum of $MA_3Bi_2Br_9$.

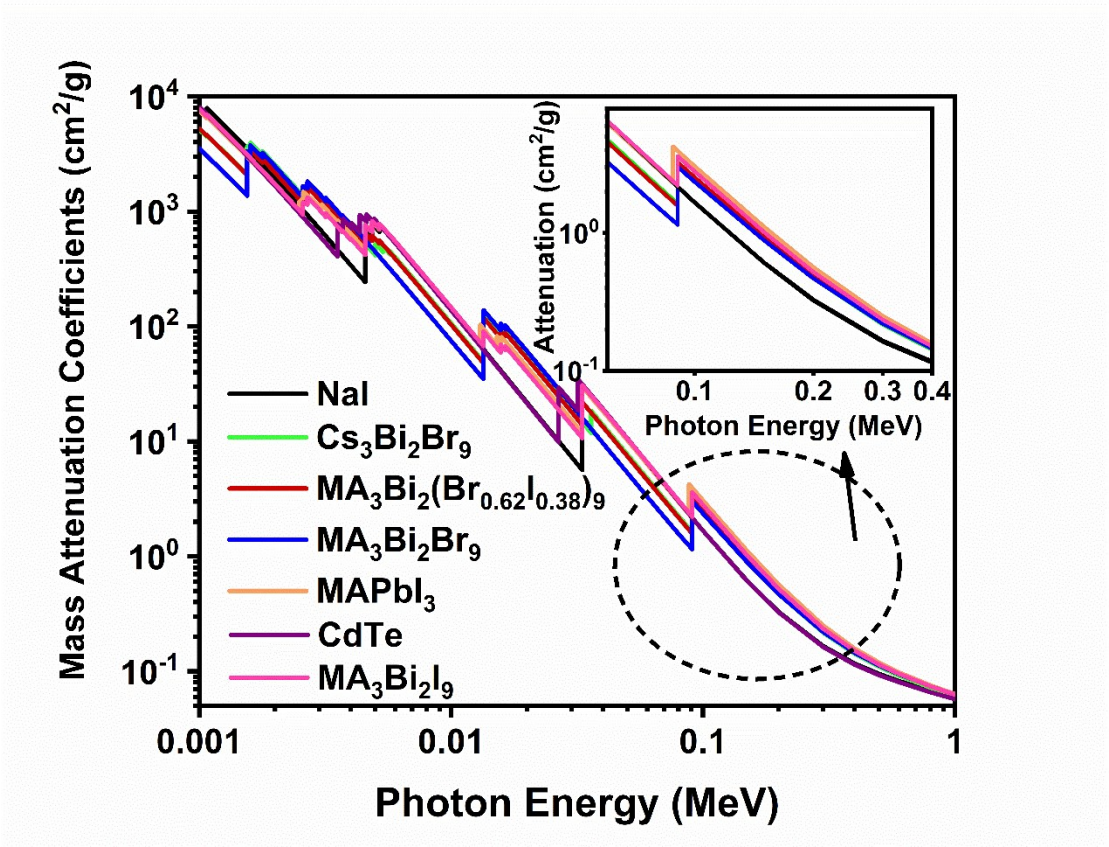

Figure S10. Mass attenuation coefficients of $MA_3Bi_2Br_9$, $MA_3Bi_2(Br_{0.62}I_{0.38})_9$, $MA_3Bi_2I_9$, and some other typical perovskite crystals. Insert present the detailed attenuation coefficients of the crystals.

Table S1. XPS results of the targeted $MA_3Bi_2X_9$ single crystals.

XPS	C	N	Bi	Br	I	SUM
$MA_3Bi_2Br_9$	22.53	13.14	12.80	51.53	0	100
$MA_3Bi_2(Br_{0.74}I_{0.26})_9$	24.04	13.21	11.47	38.75	12.53	100
$MA_3Bi_2(Br_{0.62}I_{0.38})_9$	23.56	13.02	11.67	31.79	19.96	100
$MA_3Bi_2I_9$	21.44	11.47	13.07	54.02	0	100

Table S2. Atomic coordinates ($\times 10^4$) and equivalent isotropic displacement parameters ($Å^2 \times 10^3$) for $MA_3Bi_2Br_9$.

	x	*y*	*z*	U(eq)
Bi(1)	6667	3333	6823(1)	54(1)
Br(1)	8276(4)	6547(4)	8335(3)	92(1)
Br(2)	5000	5000	5000	119(2)
C(1)	6500(300)	2540(140)	2170(100)	110(30)
N(2)	9600(300)	10400(300)	4470(80)	110(30)
N(1)	6900(200)	4220(120)	1370(100)	110(30)
C(2)	9000(200)	11000(200)	5650(110)	120(30)

$U_{(eq)}$ is defined as one third of the trace of the orthogonalized U^{ij} tensor.

Table S3. Atomic coordinates ($\times 10^4$) and equivalent isotropic displacement parameters ($Å^2 \times 10^3$) for $MA_3Bi_2(Br_{0.62}I_{0.38})_9$.

	x	*y*	*z*	U(eq)
Bi(1)	13333	6667	3169(1)	33(1)
Br(1)	15000	10000	5000	76(1)
N(1)	13333	6667	-1050(40)	220(20)
C(1)	13333	6667	-2460(40)	210(20)
Br(2)	11730(30)	3550(20)	1554(17)	59(1)
I(2)	11638(16)	3232(11)	1750(9)	59(1)
N(2)	10000	10000	5000	210(30)
C(2)	10309	8800	5876	210(40)

$U_{(eq)}$ is defined as one third of the trace of the orthogonalized U^{ij} tensor.

Table S4. Bond lengths [Å] and angles [°] for $MA_3Bi_2Br_9$.

Bi(1)-Br(1)#1	2.718(3)
Bi(1)-Br(1)	2.718(3)
Bi(1)-Br(1)#2	2.718(3)
Bi(1)-Br(2)#2	2.9672(18)
Bi(1)-Br(2)#1	2.9672(18)
Bi(1)-Br(2)	2.9672(18)
C(1)-N(1)	1.458(10)
N(2)-C(2)	1.462(10)
Br(1)#1-Bi(1)-Br(1)	92.41(11)
Br(1)#1-Bi(1)-Br(1)#2	92.41(11)
Br(1)-Bi(1)-Br(1)#2	92.41(11)
Br(1)#1-Bi(1)-Br(2)#2	90.39(8)
Br(1)-Bi(1)-Br(2)#2	175.91(8)
Br(1)#2-Bi(1)-Br(2)#2	90.45(8)
Br(1)#1-Bi(1)-Br(2)#1	90.45(8)
Br(1)-Bi(1)-Br(2)#1	90.39(8)
Br(1)#2-Bi(1)-Br(2)#1	175.91(8)
Br(2)#2-Bi(1)-Br(2)#1	86.61(6)
Br(1)#1-Bi(1)-Br(2)	175.91(8)
Br(1)-Bi(1)-Br(2)	90.45(8)
Br(1)#2-Bi(1)-Br(2)	90.39(8)
Br(2)#2-Bi(1)-Br(2)	86.61(6)
Br(2)#1-Bi(1)-Br(2)	86.61(6)
Bi(1)#3-Br(2)-Bi(1)	180

Symmetry transformations used to generate equivalent atoms:
#1 -x+y+1, -x+1, z #2 -y+1, x-y, z #3 -x+1, -y+1, -z+1

Table S5. Bond lengths [Å] and angles [°] for $MA_3Bi_2(Br_{0.62}I_{0.38})_9$.

Bi(1)-Br(2)#1	2.795(18)
Bi(1)-Br(2)	2.795(19)
Bi(1)-Br(2)#2	2.795(19)
Bi(1)-I(2)#2	2.870(9)
Bi(1)-I(2)	2.870(9)
Bi(1)-I(2)#1	2.870(9)
Bi(1)-Br(1)	3.0502(6)
Bi(1)-Br(1)#2	3.0502(6)
Bi(1)-Br(1)#1	3.0502(6)
N(1)-C(1)	1.458(10)

N(2)-C(2)	1.4592(2)
Br(2)#1-Bi(1)-Br(2)	88.1(4)
Br(2)#1-Bi(1)-Br(2)#2	88.1(4)
Br(2)-Bi(1)-Br(2)#2	88.1(4)
Br(2)#1-Bi(1)-I(2)#2	91.6(5)
Br(2)-Bi(1)-I(2)#2	93.2(6)
Br(2)#2-Bi(1)-I(2)#2	6.0(4)
I(2)#2-Bi(1)-I(2)	96.3(2)
Br(2)#1-Bi(1)-I(2)#1	6.0(4)
Br(2)-Bi(1)-I(2)#1	91.6(5)
Br(2)#2-Bi(1)-I(2)#1	93.2(6)
I(2)#2-Bi(1)-I(2)#1	96.3(2)
I(2)-Bi(1)-I(2)#1	96.3(2)
Br(2)#1-Bi(1)-Br(1)	92.5(4)
Br(2)-Bi(1)-Br(1)	178.2(4)
Br(2)#2-Bi(1)-Br(1)	93.6(4)
I(2)#2-Bi(1)-Br(1)	88.5(2)
I(2)-Bi(1)-Br(1)	172.41(17)
I(2)#1-Bi(1)-Br(1)	88.9(2)
Br(2)#1-Bi(1)-Br(1)#2	93.6(4)
Br(2)-Bi(1)-Br(1)#2	92.5(4)
Br(2)#2-Bi(1)-Br(1)#2	178.2(4)
I(2)#2-Bi(1)-Br(1)#2	172.41(17)
I(2)-Bi(1)-Br(1)#2	88.9(2)
I(2)#1-Bi(1)-Br(1)#2	88.5(2)
Br(1)-Bi(1)-Br(1)#2	85.753(19)
Br(2)#1-Bi(1)-Br(1)#1	178.2(3)
Br(2)-Bi(1)-Br(1)#1	93.6(4)
Br(2)#2-Bi(1)-Br(1)#1	92.5(4)
Br(1)-Bi(1)-Br(1)#1	85.753(19)
Br(1)#2-Bi(1)-Br(1)#1	85.753(19)
Bi(1)-Br(1)-Bi(1)#3	180

Symmetry transformations used to generate equivalent atoms:
#1 -x+y+2, -x+2, z #2 -y+2, x-y, z #3 -x+3, -y+2, -z+1

Table S6. Anisotropic displacement parameters ($Å^2 \times 10^3$) for $MA_3Bi_2Br_9$.

	U^{11}	U^{22}	U^{33}	U^{23}	U^{13}	U^{12}
Bi(1)	47(1)	47(1)	68(1)	0	0	23(1)
Br(1)	94(2)	71(2)	103(2)	-33(1)	-16(2)	35(1)
Br(2)	121(3)	119(3)	146(4)	17(3)	-17(3)	81(3)
C(1)	110(30)	110(30)	100(40)	9(16)	-1(17)	50(20)
N(2)	110(40)	110(40)	120(30)	9(16)	-10(16)	60(20)
N(1)	110(30)	110(30)	110(30)	8(16)	0(17)	50(20)
C(2)	120(40)	120(40)	120(30)	7(16)	-7(16)	50(20)

The anisotropic displacement factor exponent takes the form: $-2\pi^2[h^2a^{*2}U^{11} + ... + 2hka^*b^*U^{12}]$

Table S7. Anisotropic displacement parameters ($Å^2 \times 10^3$) for $MA_3Bi_2(Br_{0.62}I_{0.38})_9$.

	U^{11}	U^{22}	U^{33}	U^{23}	U^{13}	U^{12}
Bi(1)	30(1)	30(1)	39(1)	0	0	15(1)
Br(1)	88(2)	47(1)	81(2)	-30(1)	-15(1)	24(1)
N(1)	210(20)	210(20)	230(30)	0	0	107(11)
C(1)	210(20)	210(20)	210(30)	0	0	104(11)
Br(2)	72(1)	37(3)	61(3)	-7(2)	-6(2)	21(2)
I(2)	72(1)	37(3)	61(3)	-7(2)	-6(2)	21(2)
N(2)	210(40)	210(40)	210(40)	-10(30)	10(30)	100(30)
C(2)	210(40)	210(50)	210(40)	-10(30)	10(30)	100(30)

The anisotropic displacement factor exponent takes the form: $-2\pi^2[h^2a^{*2}U^{11} + ... + 2hka^*b^*U^{12}]$

Table S8. Bond valence of Bi cations and the distortion parameter Δd of $[BiBr_6]^{3-}$ octahedra in $MA_3Bi_2Br_9$.

	Bond length (Å)	**Bond valence**	**Bond angle (°)**	***Δd* parameter**
Bi-Br1	2.718(4)	0.766	175.9	0.75
Bi-Br2	2.967(2)	0.391		
Bi-Br1	2.718(4)	0.766	175.9	
Bi-Br2	2.967(2)	0.391		
Bi-Br1	2.718(4)	0.766	175.9	
Bi-Br2	2.967(2)	0.391		
		BVS=3.474		